

Equinoctial spread-F occurrence at low latitudes in different longitude sectors under moderate and high solar activity



M. Pietrella^{a,*}, M. Pezzopane^a, P.R. Fagundes^b, R. de Jesus^c, P. Supnithi^d, S. Klinngam^d, R.G. Ezquer^{e,f,h}, M.A. Cabrera^{e,g}

^a Istituto Nazionale di Geofisica e Vulcanologia, Rome, Italy

^b Laboratório de Física e Astronomia, Universidade do Vale do Paraíba (UNIVAP), São José dos Campos, São Paulo, Brazil

^c Instituto Nacional de Pesquisas Espaciais (INPE), São José dos Campos, São Paulo, Brazil

^d Faculty of Engineering, King Mongkut's Institute of Technology Ladkrabang (KMITL), Bangkok 10520, Thailand

^e CIASUR, Facultad Regional Tucumán, Universidad Tecnológica Nacional, Argentina

^f Laboratorio de Ionósfera, Universidad Nacional de Tucumán, Argentina

^g Laboratorio de Telecomunicaciones, Universidad Nacional de Tucumán, Argentina

^h Consejo Nacional de Investigaciones Científicas y Técnicas, Buenos Aires, Argentina

ARTICLE INFO

Keywords:

Ionosphere

Equatorial ionosphere

Ionospheric irregularities

Wave propagation

ABSTRACT

A comparative study aimed to investigate the equatorial and low-latitude spread-F occurrences for moderate solar activity (MSA) and high solar activity (HSA), was carried out considering concurrent observations made in some ionospheric stations, which identify three separate longitudinal sectors: Chiang Mai (CGM; 18.8° N, 98.9° E, mag. Lat. 13.2° N) and Chumphon (CPN; 10.7° N, 99.4° E, mag. Lat. 3.2° N), Thailand; Palmas (PAL; 10.2° S, 311.8° E, mag. Lat. 0.9° S) and São José dos Campos (SJC; 23.2° S, 314.1° E, mag. Lat. 14.0° S), Brazil; Tucumán (TUC; 26.9° S, 294.6° E, mag. Lat. 16.8° S), Argentina.

Spread-F phenomena recorded during the equinoctial months of September and October 2010, March and April 2011, for MSA, March and April 2014, September and October 2014, for HSA, were classified in two different modes: range spread-F (RSF) and frequency spread-F (FSF). The satellite trace (ST) occurrence was also investigated as possible precursor of spread-F events. When comparing the results of equatorial (CPN and PAL) and low-latitude (CGM, SJC, and TUC) stations, some common features independently of the solar activity emerge: (1) a prevalence of RSF signatures is observed in the time interval 20:00–03:00 LT, while FSF occurrences prevail in the time interval 03:00–06:00 LT; (2) STs are confirmed to be a possible precursor of RSF occurrences.

For HSA, at equatorial latitudes, spread-F occurrences in the Thai sector (CPN) are higher than those observed in the Brazilian sector (PAL).

When comparing the results of low-latitude stations of CGM, SJC, and TUC some unusual aspects characterizing the morphology of spread-F occurrences emerge: (1) contrary to the Thai and Argentine sectors, in the Brazilian sector (SJC), RSF and FSF appearances in September, for HSA, are observed with relatively long persistence times between about 03:00–06:00 LT and 01:00–03:00 LT respectively, while balanced RSF and FSF occurrences with short persistence times are observed for months for MSA; (2) a prevalence of FSF at CGM during the first half of September for MSA, never observed in the Brazilian and Argentine areas.

During years of LSA and MSA common morphological aspects are found at CGM and SJC, that is a predominance of FSF, with the lowest persistence times characterizing SJC. This suggests that the low-latitude behaviour of spread-F occurrences, under different levels of solar activity, at least in the longitude sectors here analysed, can be to a some extent generalized.

1. Introduction

The term spread-F was coined to indicate a so widespread echo trace,

in either frequency or range, that it is very hard, if not impossible, to determine the value of the F2-layer critical frequency (f_oF_2) on the ionogram. It occurs when an adequate power returns from multiple

* Corresponding author.

E-mail address: marco.pietrella@ingv.it (M. Pietrella).

Table 1

Available (A) and not available (NA) data are indicated for each station and epoch considered; the solar activity level expressed in terms of the smoothed sunspot number R_{12} is also given.

Station	CGM	CPN	PAL	SJC	TUC
Month Year/Solar activity					
September 2010/ $R_{12} = 29.5$ (MSA)	A	NA	A	A	A
October 2010/ $R_{12} = 34.5$ (MSA)	A	NA	A	A	A
March 2011/ $R_{12} = 53.8$ (MSA)	A	NA	A	A	A
April 2011/ $R_{12} = 61.1$ (MSA)	A	NA	NA	A	A
March 2014/ $R_{12} = 114.3$ (HSA)	A	A	A	A	A
April 2014/ $R_{12} = 116.4$ (HSA)	A	A	A	A	A
September 2014/ $R_{12} = 101.9$ (HSA)	A	A	A	A	A
October 2014/ $R_{12} = 97.3$ (HSA)	A	A	A	A	A

reflection paths, caused by plasma instabilities, at the same incident frequency. It is now widely agreed that the gravitational Rayleigh-Taylor (RT) instability process (Ossakow, 1981; Kelley, 2009), in conjunction with the effects of the pre-reversal enhancement (PRE) $E \times B$ drift (Kelley, 1989; Sultan, 1996; Abdu, 2001), are the basic factors to consider for the formation mechanism of the equatorial spread-F (ESF). In fact, the PRE in the zonal equatorial electric field (Kelley et al., 2009), developing at F region heights after sunset (Fejer et al., 1999), gives rise to an intense $E \times B$ drift which causes an uplifting of the ionosphere. As consequence, during nighttime hours, this process, also due to the combined action of the vertical $E \times B$ velocity and the chemical

recombination of the E and F region, leads the bottomside plasma density gradient of the equatorial F region to become steeper (Kelley, 1989; Hysell, 2000), making easier to the RT instability process to form irregularities and inhomogeneities with scale sizes from meters to hundreds of kilometers, which are responsible for ESF phenomena. Generally, four main types of spread-F can be categorized: range spread-F (RSF), frequency spread-F (FSF), mixed spread-F (MSF), and strong range spread-F (SSF).

The additional traces appearing on the ionograms as one or more quasi replicas of the F layer are known as satellite traces (STs) (Lyon et al., 1961; Rastogi, 1977; Abdu et al., 1981); they are likely produced by the presence of obliquely tilted iso-electron density surfaces caused by large scale wave structures (LSWSs) in the bottomside F layer. In the ionograms obtained at close time intervals, STs often appear before the onset of an ESF event. Therefore, STs can be regarded as an ionogram signature of LSWSs and a precursor of the ESF occurrence (Tsunoda, 2008). To this regard, Zhu et al. (2015) analysing spread-F ionograms and satellite traces over the Chinese low-latitude station of Sanya (18.0° N, 109.0° E), have found a good correlation between the occurrences of equinoctial RSF and STs, though RSF signatures do not always occurred while the ST was observed near sunset. A similar scenario was reported by Narayanan et al. (2014) from the Indian sector. On the other hand, recent studies have shown that LSWSs related to the propagation of gravity waves, can also play an important role in the ESF occurrences (Abdu et al., 2009; Cabrera et al., 2010; Krall et al., 2013 and references therein). The importance of gravity waves in concurring to the formation of daytime spread-F at low latitudes, was also recently confirmed by Jiang et al. (2016). In addition to gravity waves, also planetary wave

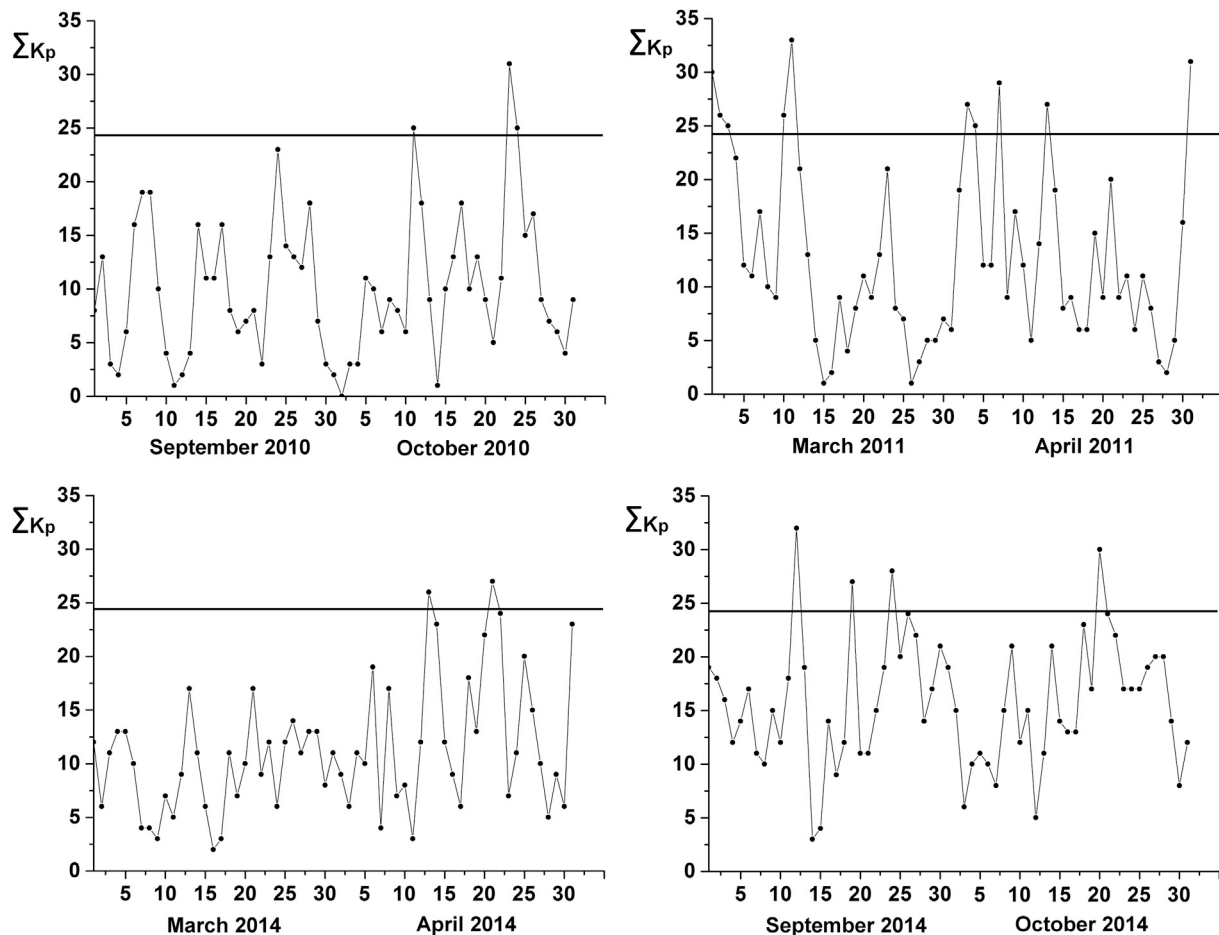


Fig. 1. Geomagnetic activity expressed in terms of ΣK_p for September and October 2010, March and April 2011, March, April, September and October 2014. The horizontal line marks the level 24 under which magnetic conditions can be considered quiet.

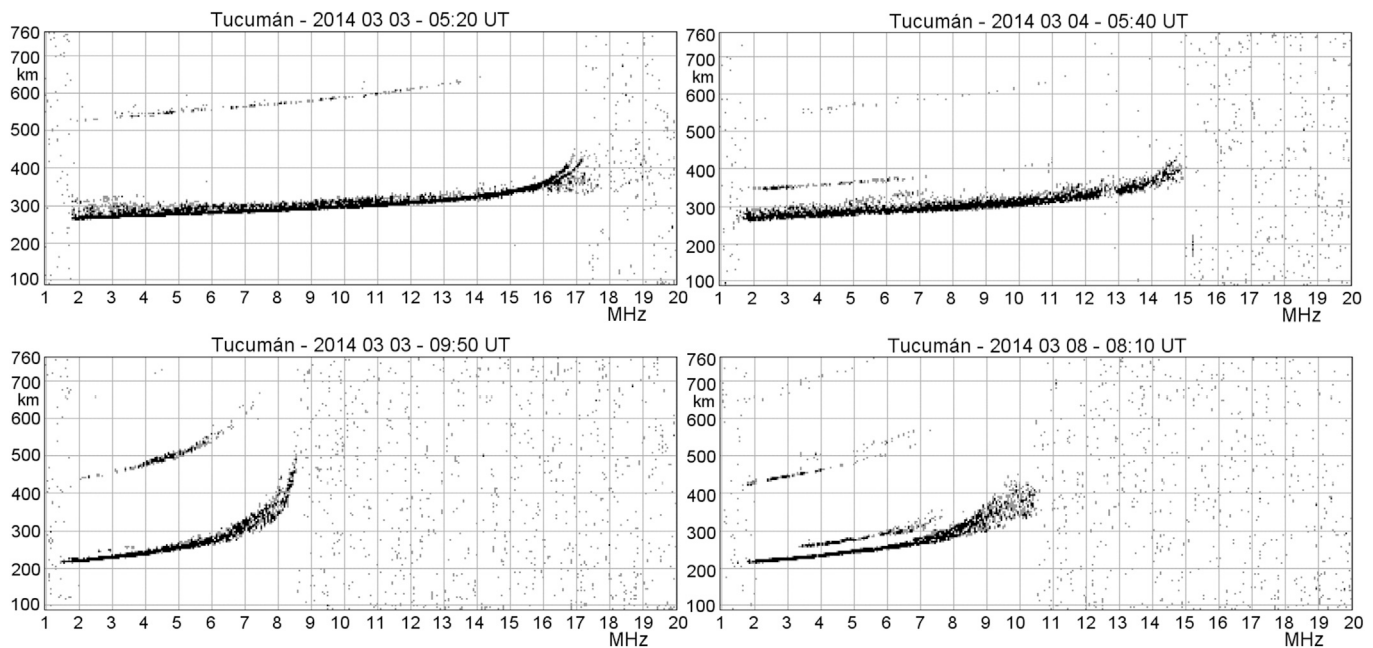


Fig. 2. Examples of RSF (top panels) and FSF (bottom panels) traces recorded at Tucumán. Both ionograms on the right are characterized by the presence of satellite traces.

scale oscillations modulating the equatorial evening PRE zonal electric field, can cause important effects on the ESF variability (Abdu et al., 2006; Fagundes et al., 2009; Bertoni et al., 2011).

The interlink between the pre-reversal $\mathbf{E} \times \mathbf{B}$ drift and the asymmetry (I_a) of equatorial ionization anomaly (EIA) was also studied to investigate the effects on the ESF occurrence, and it was found that values of $\mathbf{E} \times \mathbf{B} > 20$ m/s and $I_a < 0.3$ represent the most suitable conditions for the development of ESF occurrences in summer and equinoctial months (Lee et al., 2005).

From the existing literature it emerges that in the last decades the statistical properties of ESF phenomena have been extensively studied in terms of ESF occurrence, under different seasonal, latitudinal, longitudinal, solar and magnetic conditions. Higher ESF occurrence probabilities have been observed during summer and equinoctial months, in both hemispheres, at the low-mid latitude station of Delhi (28.6° N, 77.2° E), India, and at Jicamarca (12.0° S, 76.9° W), Peru, a low-latitude station situated near the geomagnetic equator (Lee et al., 2005; Upadhyaya and Gupta, 2014). Similar results have been found over the low-latitude Chinese station of Sanya (18.0° N, 109.0° E), with spread-F peaks at post sunset and post-midnight during equinox and summer months respectively, with occurrences of RSF and FSF comparable in summer months (Zhu et al., 2015). The analysis of ionosonde data recorded over the anomaly crest station of Ahmedabad (23.0° N, 72.4° E) and the equatorial station of Kodaikanal (10.2° N, 77.5° E), carried out to investigate the latitudinal behaviour of ESF occurrence in the Indian sector, has shown that the occurrence rate and duration of spread-F increases as we move toward the geomagnetic equator because the formation mechanism of spread-F acts more effectively at equatorial belt (Upadhyaya and Gupta, 2014). Several comparative studies have been also made to investigate possible longitudinal variations in the ESF occurrence, and several studies showed that the ESF occurrences over the longitude Brazilian sector are relatively higher than those observed over the Southeast Asian and Indian longitude sectors (Chandra et al., 2003; Hoang et al., 2010; Pezzopane et al., 2013).

Concerning the solar activity influence on spread-F phenomena, widely varied results emerge: a) higher percentage of spread-F occurrences was observed for low solar activity conditions at the low-mid latitude station of Delhi (Upadhyaya and Gupta, 2014), and at the low-latitude station of Hainan (19.5° N, 109.1° E); b) the RSF occurrence was observed to increase with the solar activity during equinoctial and

summer months, while for the FSF occurrence no relationship with the solar activity was observed (Wang et al., 2010); c) the results obtained analyzing data recorded at Cachoeira Paulista (22.5° S, 45.0° W) and Ahmedabad (23.0° N, 72.4° E), located over the anomaly crest regions in the Brazilian and Indian longitude sectors respectively, show that at Cachoeira Paulista the seasonal RSF occurrence pattern peaks in local summer both for low and high solar activity levels, while at Ahmedabad RSF occurrence probabilities showed a maximum at equinoxes and in summer during high and low sunspot years respectively (Chandra et al., 2003). Inverse relationships have been found between spread-F phenomena and magnetic activity by many authors (Rama Rao and Rao, 1961; Chandra and Rastogi, 1972). This inverse association was confirmed with a high level of statistical significance by Bowman (1995, 1998). Lee et al. (2005) found that ESF occurrences decrease with increasing K_p during equinoctial and winter months, and this feature was also confirmed by later studies, which have shown that all types of equatorial spread-F are generally suppressed in each season by an increased magnetic activity (Wang et al., 2010). Well defined inverse relationships between spread-F phenomena and magnetic activity were also found analyzing data from airglow, satellites, and scintillations (Sobral et al., 2002; Su et al., 2006; Ray and DasGupta, 2007).

Recently, a study aimed to investigate the equatorial and low-latitude spread-F occurrences at different longitude sectors was carried out by Pezzopane et al. (2013) considering the equinoctial months of March, April, September, and October 2009, characterized by low solar activity (LSA) conditions. As a continuation of this study, a new investigation was performed considering again ionograms recorded during equinoctial months, but for years following the 2009, hence relative to moderate solar activity (MSA) and high solar activity (HSA). As in Pezzopane et al. (2013), spread-F phenomena were classified as RSF or FSF, and also ST occurrences were carefully checked in order to assess them as possible precursor of spread-F events.

Spread-F phenomena occurrences analysed in this study are based on ionosonde observations simultaneously available in September and October 2010, March and April 2011, as representative of MSA, and March and April 2014, September and October 2014, as representative of HSA.

In the periods under investigation, the geomagnetic activity, analysed through the 3-hourly planetary magnetic index K_p , can be considered in general low.

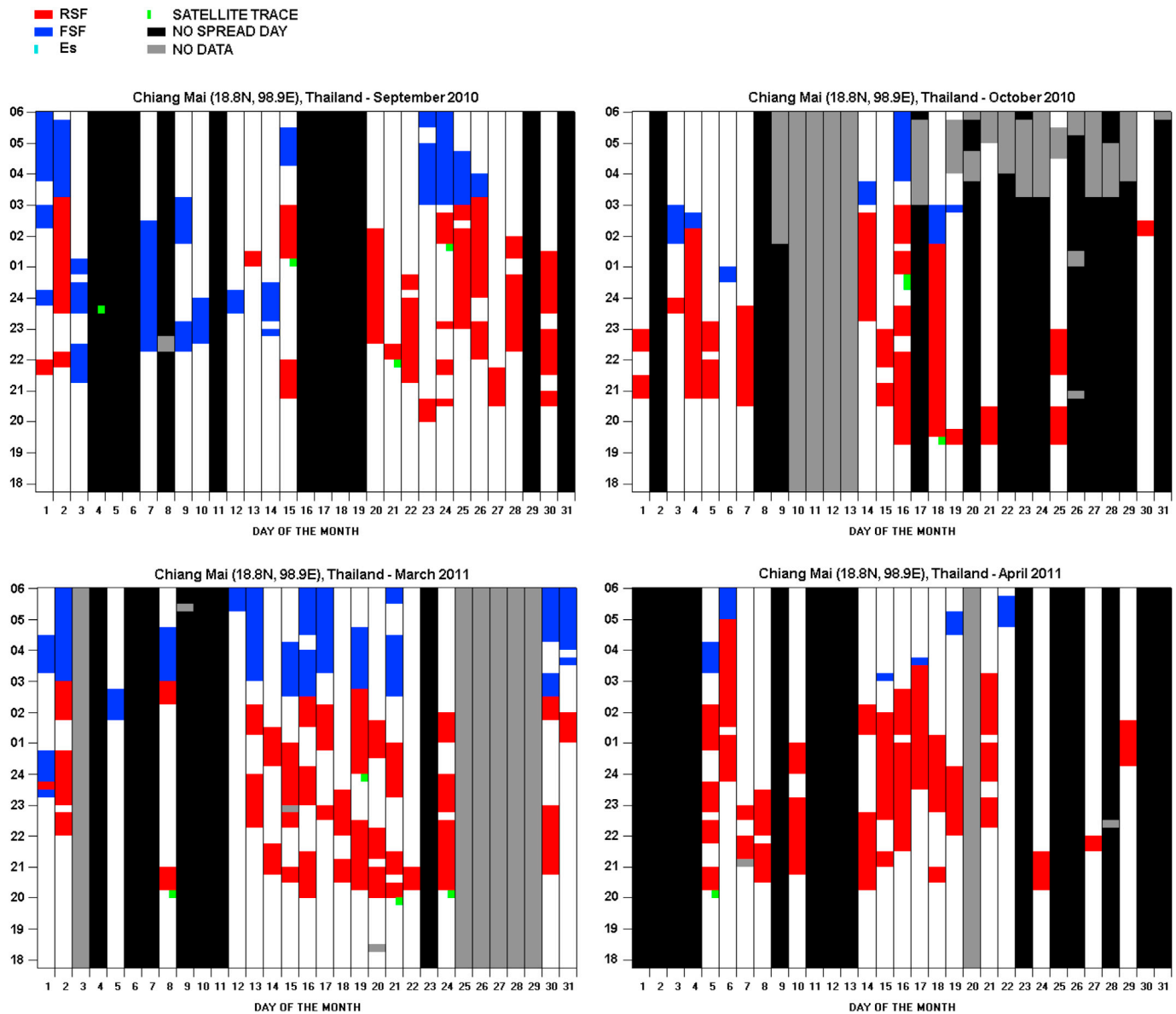


Fig. 3. Monthly patterns of RSF (red), FSF (blue), ST (green), and blanketing Es layer (cyan) occurrences at Chiang Mai for MSA. Black highlights no spread-F days. Grey highlights missing data. The y axis shows the local times. (For interpretation of the references to colour in this figure legend, the reader is referred to the web version of this article.)

Different ionospheric stations were considered, identifying three distinct longitudinal sectors: Chiang Mai (CGM; 18.8° N, 98.9° E, mag. Lat. 13.2° N) and Chumphon (CPN; 10.7° N, 99.4° E, mag. Lat. 3.2° N), identifying the Thai sector; Palmas (PAL; 10.2° S, 311.8° E, mag. Lat. 0.9° S) and São José dos Campos (SJC; 23.2° S, 314.1° E, mag. Lat. 14.0° S), identifying the Brazilian sector; Tucumán (TUC; 26.9° S, 294.6° E, mag. Lat. 16.8° S), identifying the Argentine sector. It must be noted that PAL and CPN are equatorial stations while CGM, SJC, and TUC are low-latitude stations, therefore it would have been preferable to conduct this study grouping PAL and CPN on the one hand, and CGM, SJC, and TUC on the other one, to investigate separately the possible longitudinal differences at the equatorial zone and near the EIA. Nevertheless, because of the scarcity of data at PAL for HSA, and the unavailability of data at CPN for MSA, it would not have had much sense to make comparisons between PAL and CPN. Hence the authors have sometimes preferred to include all stations when discussing spread-F occurrence patterns, without distinguishing between equatorial and low-latitude stations.

Finally, the authors would like to point out that this study was

possible thanks to a joint collaboration among different research institutes, which has requested a very large organizational effort, both to collect the huge amount of data to be analysed and for their visualization and validation, carried out not automatically but by experienced staff. As far as we know, such a large collection of RSF and FSF data, manually classified in three different longitude sectors, constitutes an exclusive database from a scientific point of view, which makes this kind of study uncommon.

Section 2 provides a description of considered data sets, and the methodology adopted to conduct the analysis. The results and the corresponding discussion are the subject of Section 3. Concluding remarks are outlined in Section 4.

2. Data sets

As the main purpose of this investigation is to carry out a comparative study of equatorial and low-latitude spread-F occurrences over the five ionospheric stations mentioned in the previous section, it is crucial for our study that the ionosonde observations are concurrently present at

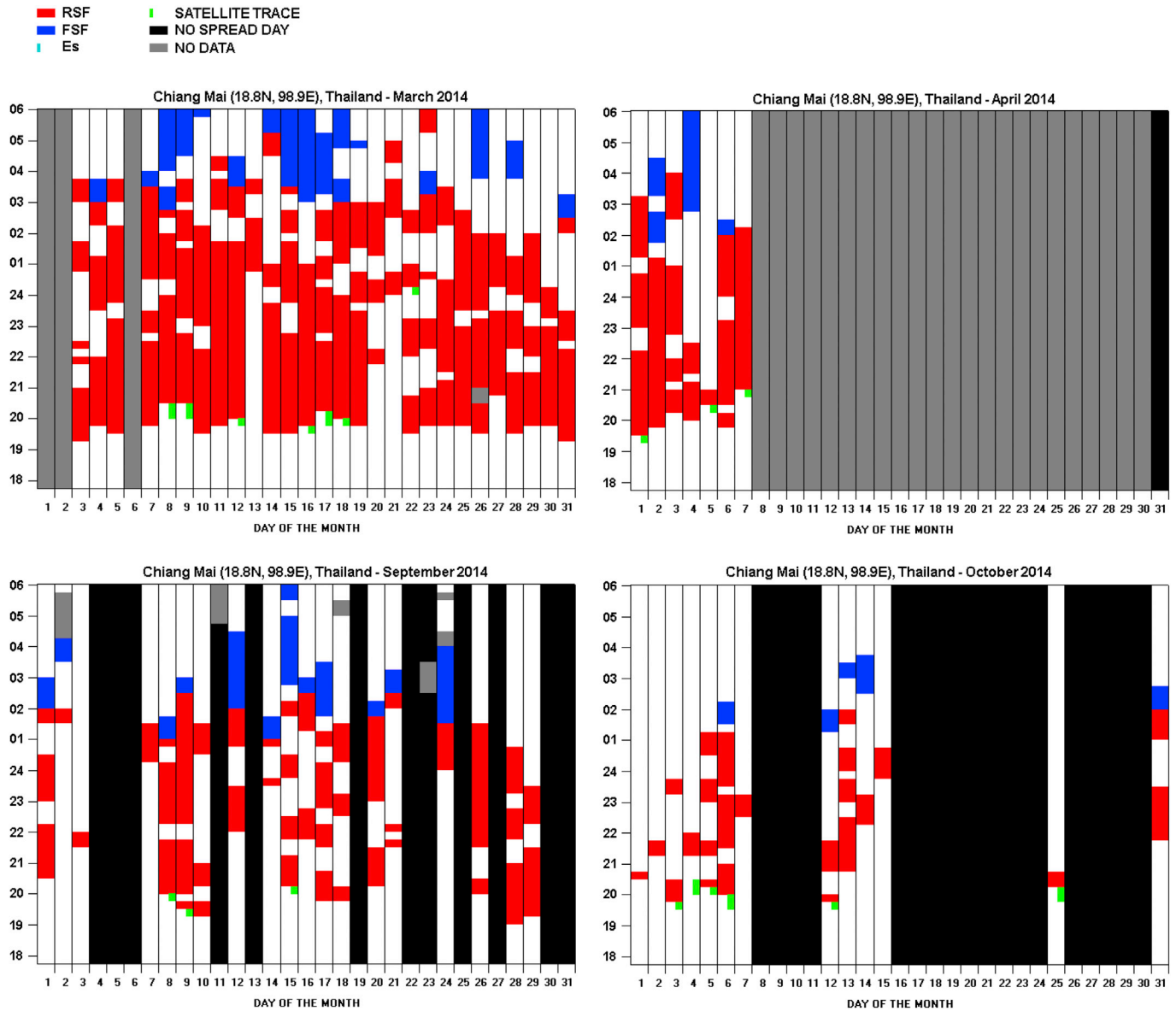


Fig. 4. Same as Fig. 3, but at Chiang Mai for HSA.

CGM, CPN, PAL, SJC, and TUC. As the equatorial and low-latitude spread-F phenomena are practically absent during daytime (e.g., Alfonsi et al., 2013), our investigation was focused on the time interval between 18:00 and 06:00 LT, i.e. during nighttime hours. For convenience, ionospheric stations and epochs involved in this study, as well as levels of solar activity expressed in terms of the smoothed sunspot number R_{12} , are summarized in Table 1.

The 3-hourly planetary geomagnetic index K_p data were also considered to test the magnetic activity conditions during the periods under investigation.

As the value 3 of the index K_p is generally considered the threshold under which magnetic conditions can be considered quiet (Bhaneja et al., 2009; Wang et al., 2010), a value of $\sum K_p \leq 24$ is usually representative of a quiet day.

We found that geomagnetic conditions can be assumed quiet for each month, because on a daily basis only sometimes $\sum K_p$ exceeds the value of 24 (Fig. 1).

The kind of ionosonde and the corresponding sounding repetition rate (SRR) are the following: an FMCW (frequency-modulated continuous wave) (Poole, 1985) ionosonde was employed to record ionograms at

CGM and CPN with a SRR equal to 15 min; a CADI (Canadian Advanced Digital Ionosonde) (McDougall, 1997) provided ionograms recorded at PAL and SJC with a SRR equal to 5 min; an AIS-INGV (Advanced Ionospheric Sounder - Istituto Nazionale di Geofisica e Vulcanologia) (Pezzopane et al., 2007) was used with a SSR equal to 10 min to obtain ionograms at TUC.

The comparative study of spread-F occurrence was conducted classifying in each site spread-F traces from the ionograms in two different modes: a) FSF, the signatures of which typically show an echo wide-spread along the frequency axis near the critical frequencies of the ordinary and extraordinary traces of the ionograms, and therefore they are associated to plasma irregularities close to the F-region peak; b) RSF, the signatures of which are characterized by an echo widespread along the height axis, and hence they are related to plasma irregularities occurring in the lower part of the F region. Since the study conducted by Pezzopane et al. (2013) for LSA proved that STs sometimes behave as a precursor of RSF occurrences, also in this investigation ST occurrences have been carefully checked in order to verify whether, under MSA and HSA, they can be again considered as a precursor of spread-F events. Some examples of FSF, RSF, and ST are shown for convenience in Fig. 2 for Tucumán.

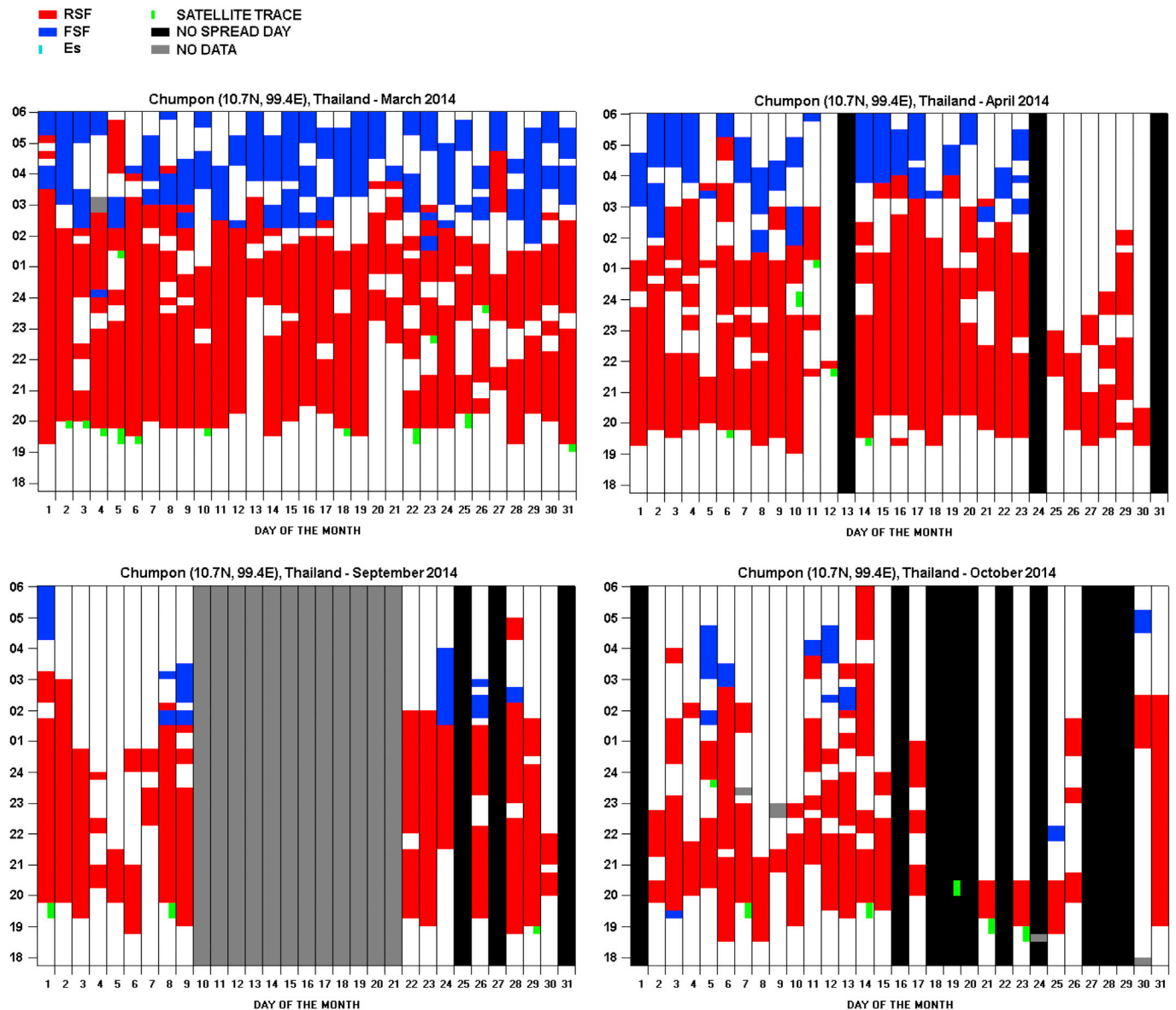


Fig. 5. Same as Fig. 3, but at Chumpon for HSA.

3. Results and discussion

Figs. 3–11 show the monthly patterns of occurrence of both spread-F types obtained from the analysis carried out in each station under study for September and October 2010, March and April 2011 (MSA), and for March, April, September, and October 2014 (HSA). The appearance of RSF and FSF events, the presence of blanketing sporadic E (Es) layer, the ST occurrence, the daily absence of spread-F phenomena, and the lack of data are marked in red, blue, cyan, green, black, and grey respectively.

The results shown in these figures were carefully analysed in order to highlight the main features related to the RSF and FSF occurrences and their differences for MSA and HSA conditions and different longitude sectors.

The outcomes for CGM (Figs. 3–4) show generally a predominance of RSF phenomena in the time interval 20:00–03:00 LT with persistence times characterizing the RSF occurrences in March for HSA, relatively longer than those observed for MSA. Generally, FSF occurrences are observed to prevail in the time interval 03:00–06:00 LT both for MSA and HSA conditions. It is noteworthy that during the first half of September, FSF occurrences for MSA prevail on the RSF ones, while the situation is

reversed for HSA when only a few FSF events are observed. The ST appearance often precedes RSF phenomena independently of the solar activity, even though they are noticed in a less extent during MSA.

Unfortunately, for CPN, data for MSA are not available, thus only the results for HSA were analysed (Fig. 5): an overwhelming majority of RSF occurrences are clearly observed in all months in the time interval 20:00–03:00 LT, with relatively long persistence times especially in March and April; FSF occurrences prevail in the time interval 03:00–06:00 LT. In March and April, some FSF events before 03:00 LT are also observed. The ST appearance oftentimes anticipates the RSF occurrence.

With regard to PAL (Figs. 6–7), it must be noted that for both MSA and HSA there exist relatively large periods for which ionosonde observations are missing: specifically, for MSA, from 22 to 31 October, from 5 to 31 March, and during the whole month of April, while for HSA, from 6 to 20 March, and for almost the whole months of September and October. Anyway, RSF occurrences are observed to prevail over the FSF ones in the time interval 20:00–03:00 LT, with relatively long persistence times in September and October, for MSA, and in March, for HSA. Even though for MSA many cases of blanketing Es prevent from detecting possible spread-F phenomena, it is however notable that in the time interval 03:00–06:00

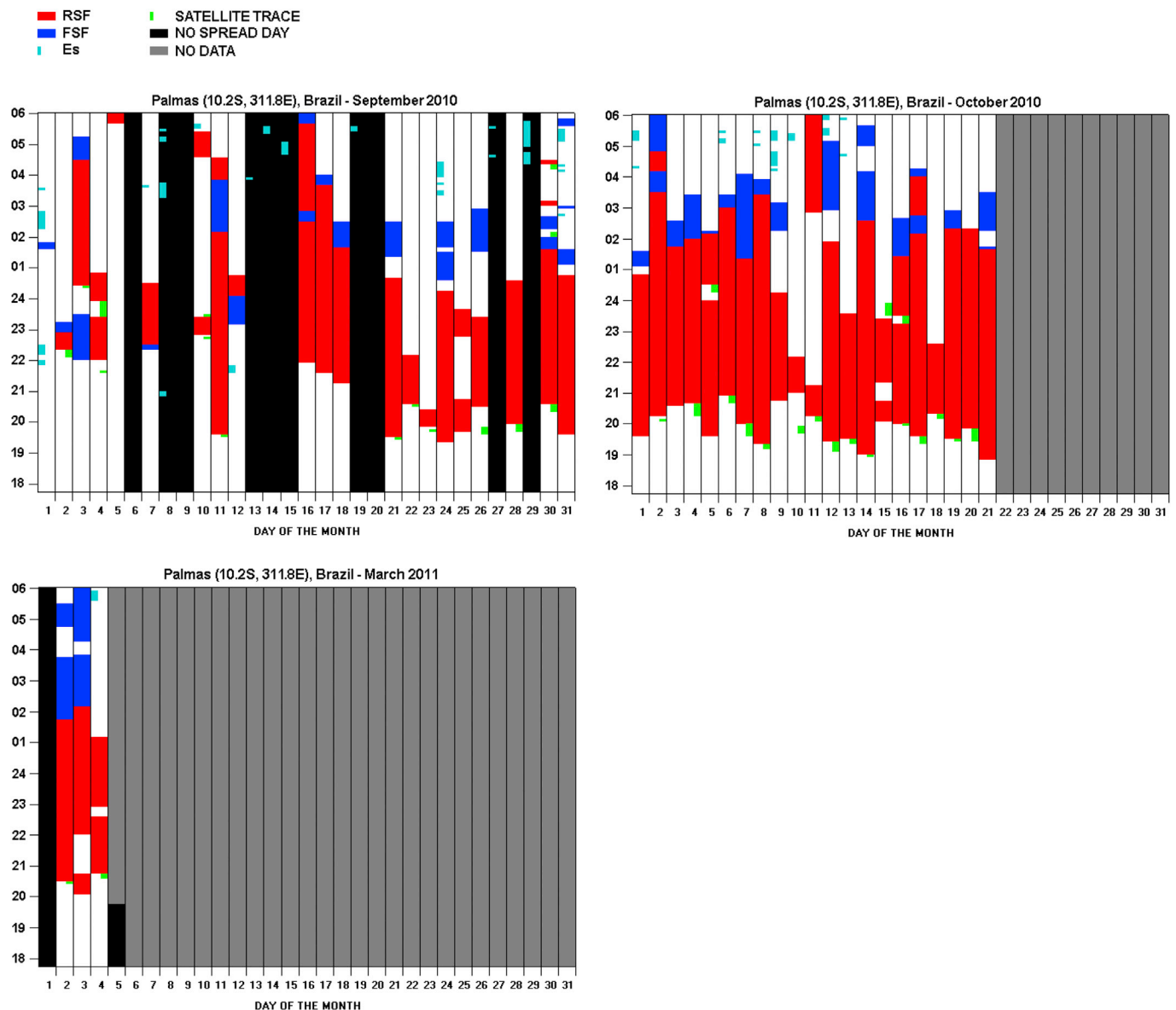


Fig. 6. Same as Fig. 3, but at Palmas for MSA. The monthly pattern for April 2011 is missing because corresponding data are not available.

LT a predominance of FSF occurrences is observed, mainly in October 2010 and March 2011, while RSF events with relatively long persistence times are sometimes noticed; several FSF signatures are however observed in September and October in the time interval 01:00–03:00 LT. In April, before 03:00 LT, many FSF events are observed also for HSA. The ST appearance often precedes the RSF event independently of the solar activity.

The results for SJC (Figs. 8–9) show that in the time interval 21:00–02:00 LT, while RSF and FSF occurrences for MSA are observed more or less in the same extent in September, October, and March, so that there is not a sharp prevalence of one spread-F type, for HSA, a predominance of RSF events is observed in March and October; independently of the solar activity, RSF occurrences are characterized by relatively short persistence times. For MSA, FSF events prevail on the RSF ones in the time interval 03:00–06:00 LT in all months, a feature that is also observed for HSA but only in March. In fact, very peculiar is the pattern observed for HSA in September, being characterized by the presence of RSF(FSF) occurrences with relatively long persistence times in the time intervals 03:00–06:00 LT(00:00–03:00 LT), respectively. In more than a few cases, STs were not

followed by RSF/FSF phenomena, indicating that LSWS may not always trigger spread-F phenomena although they can play an important role for their formation (Abdu et al., 2009; Cabrera et al., 2010; Krall et al., 2013 and references therein). It must be noted that there exist relatively large periods for which spread-F phenomena are not observed; in particular, this occurs in April, for both MSA and HSA, and from 1 to 11 September, for HSA.

With regard to TUC (Figs. 10 and 11), a large number of cases with no data and no spread-F days characterize the four monthly patterns, for MSA, and that of April, for HSA. For both MSA and HSA, a prevalence of RSF occurrences clearly appears in the time interval 20:00–03:00 LT. For HSA, FSF events prevail in the time interval 03:00–06:00 LT, and RSF occurrences are characterized by very short persistence times. Noteworthy is the absence of spread-F phenomena which characterizes many days of April independently of the solar activity. STs appear very often at TUC and strictly related with the occurrence of RSF events, for both MSA and HSA.

When comparing the equatorial and low-latitude stations, the following general features can be drawn:

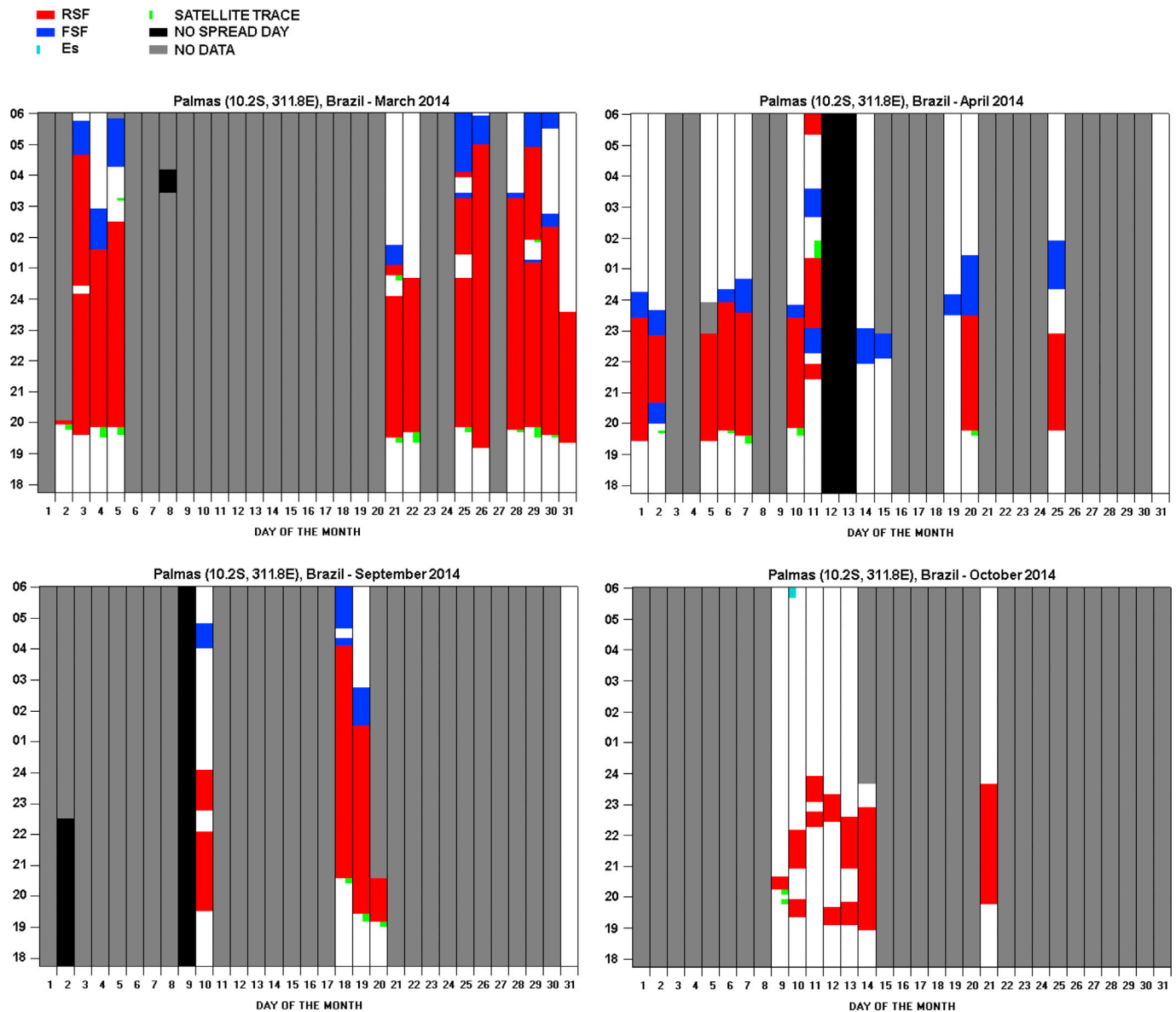


Fig. 7. Same as Fig. 3, but at Palmas for HSA.

- (1) independently of the solar activity, a prevalence of RSF signatures is observed in the time interval 20:00–03:00 LT, while FSF occurrences prevail in the time interval 03:00–06:00 LT;
- (2) independently of the solar activity, STs are confirmed to play a role as a possible precursor to the development of RSF in the Thai and Argentine sectors, and at PAL in the Brazilian sector. More deeply, other features can be observed:
- (3) independently of the solar activity, the majority of no spread-F days was found in April at SJC and TUC, the two stations nearest to the southern crest of EIA;
- (4) for HSA, spread-F occurrences over the Thai sector are significantly higher than those observed in the other sectors;
- (5) the highest spread-F occurrences are noticed at PAL in October and at CPN in March, for MSA and HSA respectively;
- (6) for HSA, at SJC and TUC, RSF occurrences in the time interval 20:00–03:00 LT show shorter persistence times than those observed at CGM, CPN, and PAL;
- (7) for MSA, an equinoctial asymmetry is observable at SJC where the spread-F occurrence is higher in September–October, as well as at TUC and CGM where the spread-F occurrence is higher in March;

given that SJC and TUC are positioned in the southern hemisphere, while CGM is located in the northern hemisphere, the equinoctial asymmetries imply also a hemispherical asymmetry. For HSA, the equinoctial asymmetry is visible at SJC, TUC, CGM, and CPN where the spread-F occurrence is higher in March.

Analysing more accurately the results illustrated in Figs. 3–11, when comparing the low-latitude stations of CGM, SJC, and TUC, additional features come out:

- (8) in the Brazilian sector, RSF and FSF signatures with relatively long persistence times are respectively noticed in the time interval 03:00–06:00 LT and 00:00–03:00 LT at SJC, in September, for HSA. These features are never observed in the Thai and Argentine longitude sectors;
- (9) FSF occurrences for MSA are higher than those occurring for HSA in the time interval 21:00–02:00 LT (see for instance the related plots for CGM in September, and for SJC in September and October);
- (10) The highest and lowest FSF occurrences for MSA are observed in the Brazilian and Argentine longitude sectors respectively; for HSA, FSF signatures are observed less frequently in the Thai

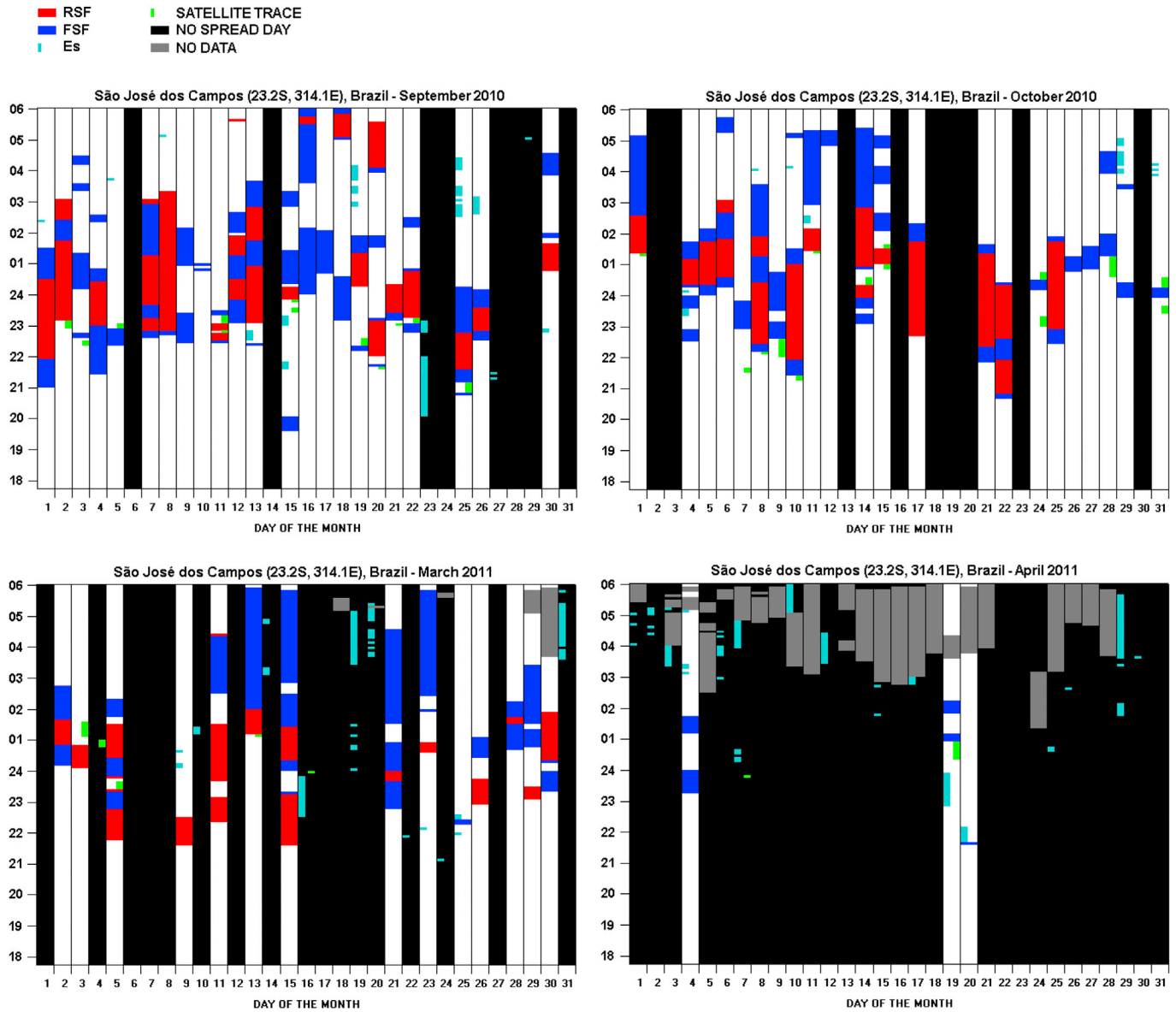


Fig. 8. Same as Fig. 3, but at Sao Jose Dos Campos for MSA.

longitude sector than in the Argentine and Brazilian ones which show somewhat balanced FSF occurrences.

- (11) for MSA, somewhat balanced RSF and FSF appearances with relatively short persistence times are found in the time interval 20:00–03:00 LT at SJC for all months. This observational feature is not observed in the Thai and Argentine longitude sectors;
- (12) for MSA, only in the Thai area, during the first two weeks of September, FSF occurrences are noticed to prevail on the RSF ones in the time interval 20:00–03:00 LT.

As already mentioned in the introduction, this paper is a continuation of a recent study carried out by Pezzopane et al. (2013) under low solar activity conditions. It must be pointed out that LSA periods analysed by Pezzopane et al. (2013), and those considered in this study, are practically geomagnetically quiet periods, because $\sum K_p$ shows values always lower than 24 (see Fig. 2 of Pezzopane et al. (2013)) and only sometimes values exceeding 24 (see Fig. 2). Some comparisons between the main results achieved by Pezzopane et al. (2013) and those arising from this investigation are here summarized:

- a) for LSA and MSA, the highest ESF occurrences are found at PAL in October, while for HSA, the highest ESF occurrences are observed at CPN in March; for LSA, ESF occurrences over the Brazilian area are significant higher than those observed over the Southeast Asian region, while the situation is reversed for HSA, when the highest ESF occurrences are noticed in the Thai zone at CPN in March–April;
- b) the predominance of RSF occurrences, recorded over the Southeast Asian and Argentine sectors for LSA, is still observed for HSA over the Southeast Asian sector, and for MSA over the Brazilian sector; also for MSA, as it occurred for LSA, FSF occurrences prevail at CGM and SJC;
- c) as it was recorded for LSA, spread-F signatures at SJC seem to appear with lower persistence times than at any other station also for MSA, while for HSA lower persistence times seem to characterize TUC;
- d) for LSA and MSA, the same equinoctial and hemispherical asymmetries are observed at SJC and CGM;
- e) as it occurred for LSA, also for MSA and HSA STs are confirmed to be a precursor for the appearance of an RSF trace in the Southeast Asian and Argentine sectors, and at PAL in the Brazilian sector; besides, ST occurrences are overall higher for HSA than for MSA and LSA;

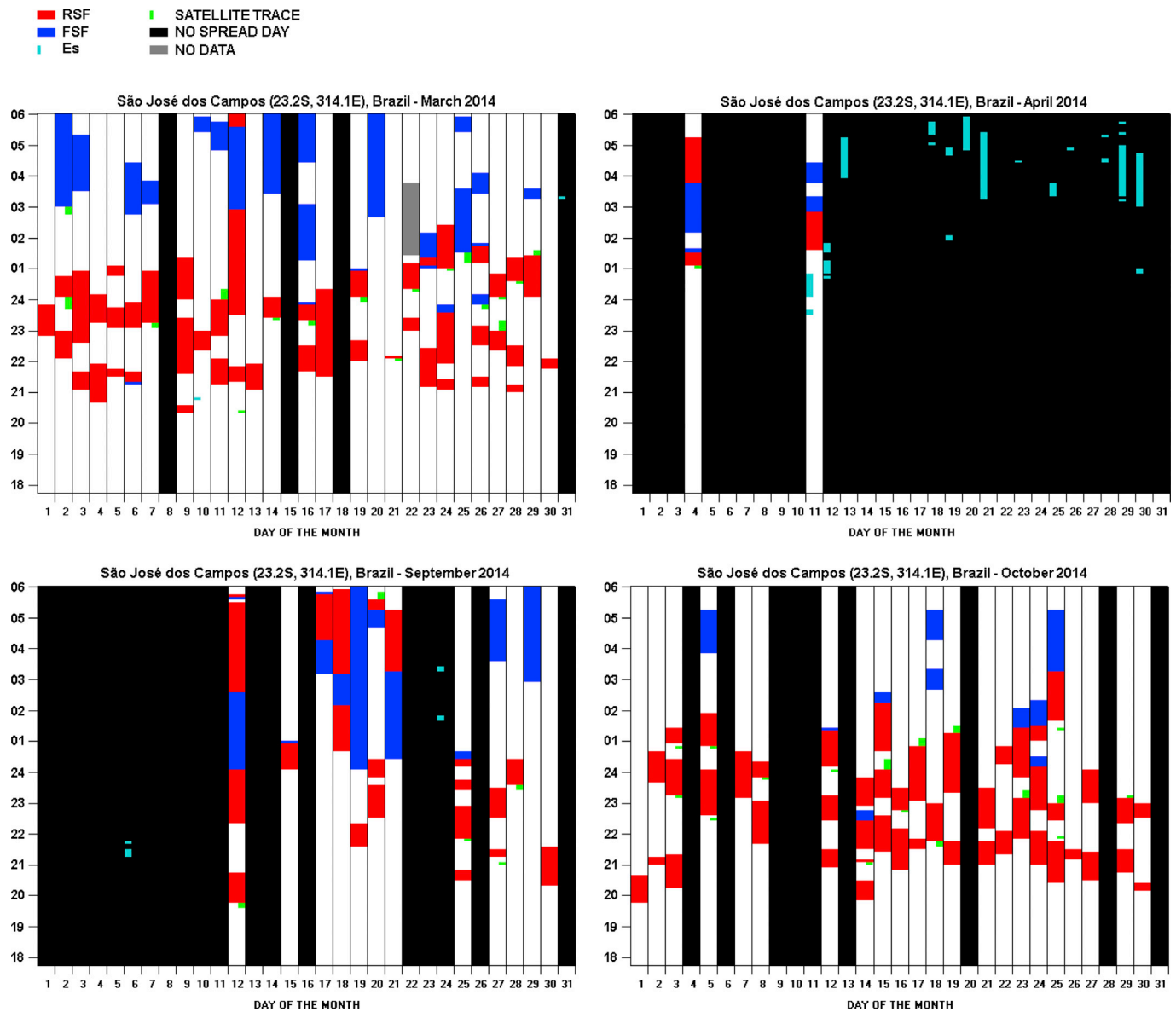


Fig. 9. Same as Fig. 3, but at Sao Jose Dos Campos for HSA.

f) while for LSA the majority of no spread-F days is found over the Southeast Asian sector, the largest number of no spread-F days was found at TUC, for MSA, and SJC, for HSA, the two south American stations nearest to the southern crest of EIA.

As already mentioned in the introduction, there are several interconnected physical mechanisms which are responsible for the development and variability of ESF phenomena: the RT instability process operating in combination with the PRE causing an uplifting of the F-layer (Fejer et al., 1999; Whalen, 2002); the steep gradient at the bottomside of the F-layer (Kelley, 1989); the gradient in the integrated E region Pedersen conductivity (Tsunoda, 1985; Stephan et al., 2002); the *trans*-equatorial component of the thermospheric winds (Maruyama and Matuura, 1984; Maruyama, 1988). Even though the causes generating ESF phenomena are to be sought among the above mentioned mechanisms, it is however not easy to justify all the results emerged from this study.

A prevalence of RSF signatures observed in the time interval 20:00–03:00 LT is indicative of irregularities which develop in the bottomside F region; these irregularities, drifting upward towards the F-region peak,

would cause later the FSF occurrences which are observed between 03:00–06:00 LT. Except in SJC, STs are confirmed to be a precursor for the appearance of an RSF, in agreement with the fact that STs are signatures of LSWS (Tsunoda, 2008) related to the propagation of gravity and planetary waves which, in turn, can play an important role in the ESF occurrences (Abdu et al., 2009; Cabrera et al., 2010; Krall et al., 2013; and references therein); in fact, LSWS can also amplify the source of irregularities during post sunset hours (Fejer et al., 1999; Hysell and Burcham, 2002; Klausner et al., 2009) and thus generating the wedges of plasma depletions which cause the RSF signatures. On the other hand, at SJC the ST appearance as precursor of the RSF occurrence can be claimed neither for MSA nor for HSA, according to the results found for LSA (Pezzopane et al., 2013).

The presence of a *trans*-equatorial component of the thermospheric wind along the magnetic meridian in the F region, which suppresses the growth of the Rayleigh-Taylor type plasma instabilities (Maruyama and Matuura, 1984), could explain the larger number of no spread-F days recorded at TUC and SJC, for MSA and HSA respectively; on the other hand, this situation is reversed to that observed for LSA, when the majority of no spread-F days is observed over the Southeast Asian sector in

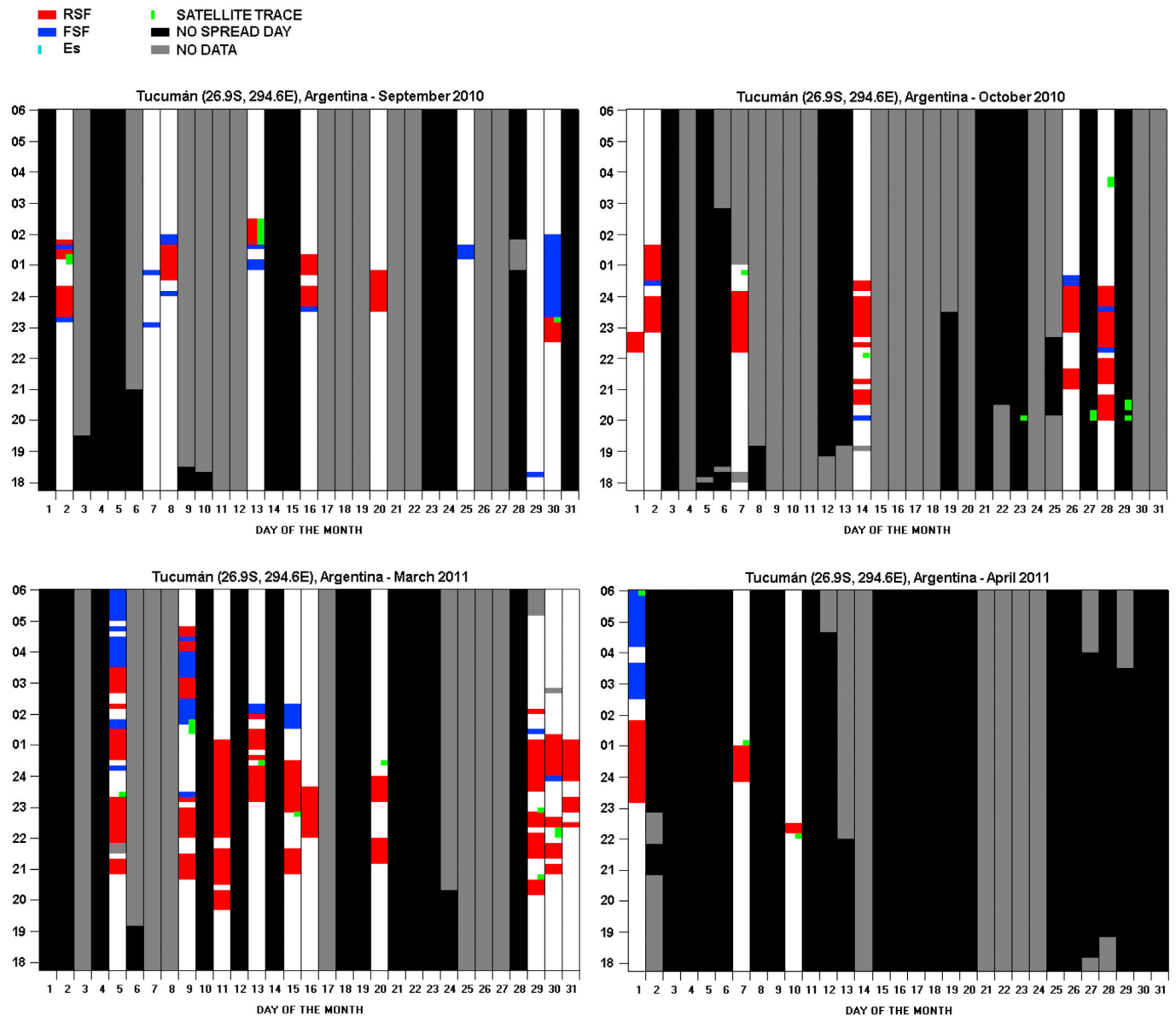


Fig. 10. Same as Fig. 3, but at Tucumán for MSA.

accordance with the results of [Abdu et al. \(2006\)](#) and [Saito and Maruyama \(2006\)](#), indicating a most pronounced suppression of spread-F events caused by meridional winds just in the Thai-Indonesian area.

Another aspect that has to be considered is that the spread-F phenomenon in the presence of a large PRE is not suppressed by a meridional wind ([Sastri et al., 1997](#)). This means that the large number of no spread-F days characterizing the Thai area for LSA (see [Pezzopane et al., 2013](#)) might be the result of smaller sunset uplifts of the F-region than those characterizing the Brazilian and Argentine area. The same physical mechanism might be at the base of the large number of no spread-F days recorded at TUC for MSA and at SJC for HSA.

Concerning the longitudinal differences, for MSA, when comparing PAL monthly patterns of September–October with those of CGM, a higher spread-F occurrence is found in the Brazilian sector. This result is probably due to different effects of the PRE and *trans*-equatorial winds which in the Southeast Asian zone are more effective in suppressing spread-F events ([Abdu et al., 2006](#); [Saito and Maruyama, 2006](#)), and it confirms the outcomes achieved by [Pezzopane et al. \(2013\)](#) for LSA. The situation appears reversed for both MSA, when comparing CGM monthly patterns with those of SJC, and for HSA, when comparing CGM and CPN monthly

patterns with those of PAL and SJC. In these cases higher spread-F occurrences are found in the Thai sector.

The fact that a meridional wind cannot suppress spread-F phenomena in presence of a large PRE ([Sastri et al., 1997](#)) suggests that, unlike what happened for LSA and MSA (comparing PAL and CGM), in the Thai zone the uplift of the F region is likely greater than that characterizing the Brazilian sector (specifically, at SJC for MSA, and at PAL and SJC for HSA), which during high sunspot years might have been characterized by a significant suppression of spread-F events caused by meridional winds.

These considerations lead us to speculate that the effectiveness of thermospheric meridional *trans*-equatorial winds in suppressing the equatorial and low-latitude plasma bubbles strongly depends on the geomagnetic latitude and longitude, and solar activity level. This is however an issue that needs to be investigated more deeply.

The mechanism involving the PRE and RT instability processes for the generation of ESF ([Basu and Kelley, 1979](#); [Kelley and McClure, 1981](#); [Ossakow, 1981](#)) acts more effectively at the geomagnetic equator. This mechanism gives rise to inhomogeneities and irregularities which develop at the bottom-side F region and often remain below the topside ([Aarons, 1993](#); [Whalen, 2002](#)), therefore they can be observed as ESF

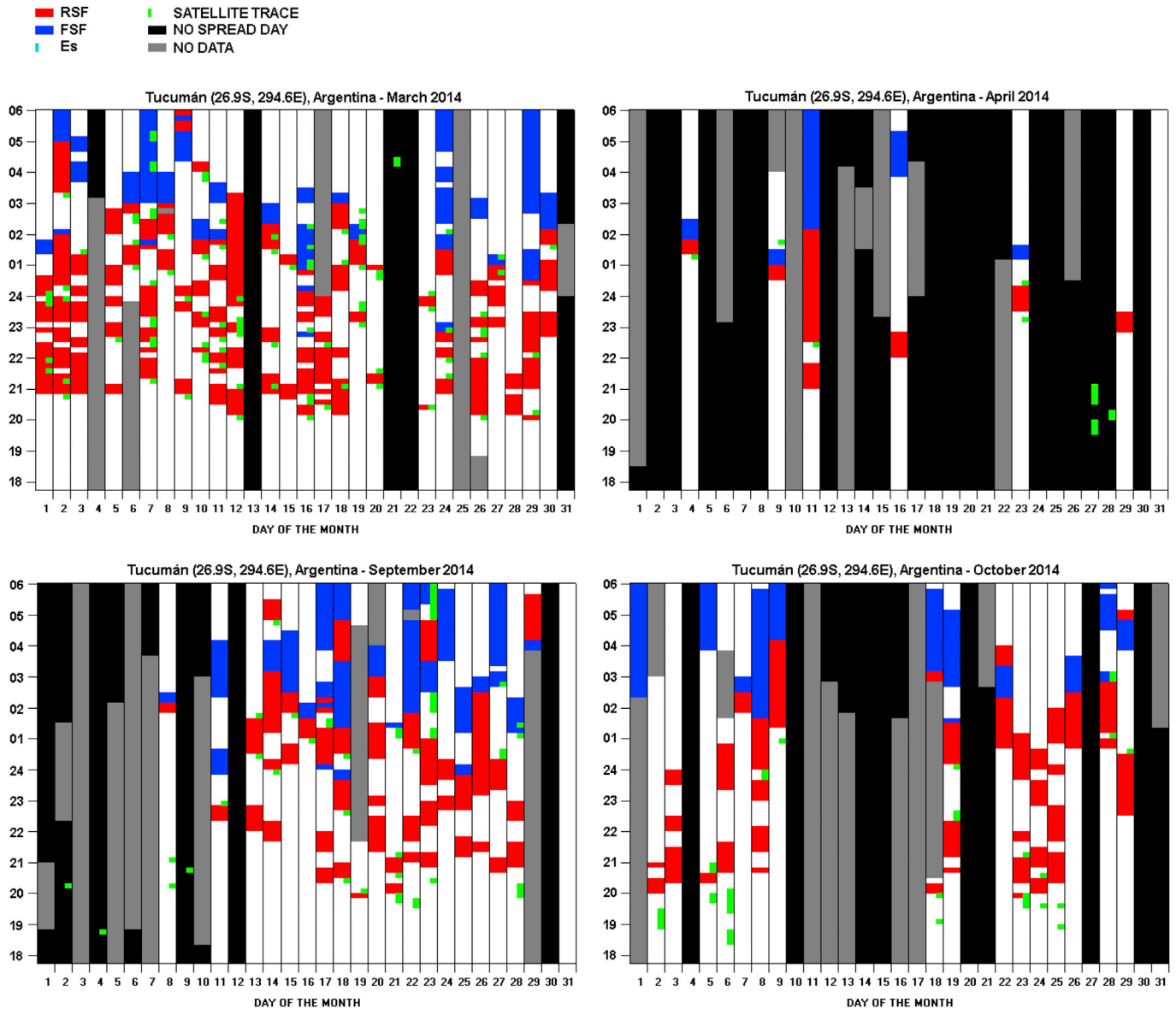


Fig. 11. Same as Fig. 3, but at Tucumán for HSA.

traces on ionograms recorded near the magnetic equator. Concerning this, the highest ESF occurrences observed for LSA and MSA at PAL in October, and for HSA at CPN in March, are compatible with this mechanism because the majority of ESF occurrences is of RSF type, hence coming from irregularities below the F-region peak; moreover, PAL and CPN are the two nearest sites to the geomagnetic equator, where the development of irregularities is more probable. This could also explain why longer persistence times are generally observed at geomagnetic low-latitude stations (CGM, CPN, and PAL) rather than at stations located near the crest of EIA (SJC and TUC).

Different sunset times occurring in the F-region to the south and north of the magnetic equator, as well as a combined action of relatively strong *trans*-equatorial neutral wind effects with the $\mathbf{E} \times \mathbf{B}$ drift on the electron density distribution (Maruyama and Matuura, 1984; Maruyama, 1988) could be responsible for the observed equinoctial and hemispherical asymmetries.

4. Summary

Equinoctial RSF and FSF occurrences were studied at equatorial and

low latitudes during moderate (September–October 2010 and March–April 2011) and high (March–April and September–October 2014) solar activity years, using ionograms simultaneously recorded at five stations which mark three well distinct longitudinal sectors: Thai, Brazilian and Argentine.

Comparisons between equatorial and low-latitude stations have shown some common features which does not depend on the solar activity: RSF and FSF are mainly observed in the range 20:00–03:00 LT and 03:00–06:00 LT respectively; STs are confirmed to be a precursor of RSF occurrences.

The highest ESF occurrences, and the longest persistence times found at stations close to the geomagnetic equator, can be explained by means of the RT instability process operating in combination with the $\mathbf{E} \times \mathbf{B}$ drift.

ESF occurrences in the Thai sector (CPN), higher than those observed in the Brazilian zone (PAL) for HSA, suggest that in the equatorial regions the combined action of *trans*-equatorial winds and the $\mathbf{E} \times \mathbf{B}$ drift has a different effectiveness depending on the longitudinal sector considered.

When comparing CGM, SJC, and TUC, unusual spread-F occurrences at low latitudes also emerge. Specifically, the observations at SJC of RSF

and FSF in September, for HSA, with relatively long persistence times between about 03:00–06:00 LT and 01:00–03:00 LT respectively, as well as the balanced RSF and FSF occurrences with short persistence times observed for all months for MSA, are peculiar features not observed in the Thai and Argentine sectors.

The prevalence of FSF at CGM during the first half of September for MSA, never observed in the Brazilian and Argentine area, is another peculiar aspect characterizing the morphology of spread-F phenomena in the Thai sector.

These observational results remain enigmatic, and point out once more that the physical processes underlying the low-latitude spread-F events development and their variability are really complex and difficult to be fully understood.

The results of this study were compared with those obtained by Pezzopane et al. (2013) who analysed spread-F occurrences over the same stations considered in this study, but for LSA.

From this comparison it was possible to identify some common features, as the prevalence of FSF occurrences at CGM and SJC, and the lowest persistence times characterizing the spread-F occurrences at SJC. Moreover, the same equinoctial and hemispherical asymmetries observed at SJC and CGM, for LSA and MSA, suggest that the low-latitude behaviour of spread-F occurrences, under different levels of solar activity, can be to a some extent generalized, at least in the longitude sectors here analysed. The prevalence of no spread-F days mostly observed in the Thai (CGM), Argentine (TUC), and Brazilian (SJC) sectors, for LSA, MSA and HSA respectively, and spread-F occurrences in the Thai sector (CGM), lower(higher) than those observed in the Brazilian sector (SJC) for LSA(MSA and HSA), suggest that the effectiveness of the joint action of meridional winds and the PRE process, in suppressing low-latitude spread-F occurrences, depends on both the solar activity and the geomagnetic latitude and longitude.

Overall the results here illustrated confirm that the features of equatorial and low-latitude spread-F phenomena can change remarkably under different seasonal, latitudinal, longitudinal, and solar conditions.

Acknowledgements

The authors are grateful to the reviewer for his comments and suggestions which have contributed to improve the paper.

References

- Aarons, J., 1993. The longitudinal morphology of equatorial F-layer irregularities relevant to their occurrence. *Space Sci. Rev.* 63, 209–243. <http://dx.doi.org/10.1007/BF00750769>.
- Abdu, M.A., Batista, I.S., Bittencourt, J.A., 1981. Some characteristics of spread F at the magnetic equatorial station Fortaleza. *J. Geophys. Res.* 86, 6836–6842. <http://dx.doi.org/10.1029/JA086iA08p06836>.
- Abdu, M.A., 2001. Outstanding problems in the equatorial ionosphere thermosphere electrodynamics relevant to spread F. *J. Atmos. Solar Terr. Phys.* 63, 869–884. [http://dx.doi.org/10.1016/S1364-6826\(00\)00201-7](http://dx.doi.org/10.1016/S1364-6826(00)00201-7).
- Abdu, M.A., Iyer, K.N., de Medeiros, R.T., Batista, I.S., Sobral, J.H.A., 2006. Thermospheric meridional wind control of equatorial spread-F and evening prereversal electric field. *Geophys. Res. Lett.* 33, L07106 <http://dx.doi.org/10.1029/2005 GL024835>.
- Abdu, M.A., Kherani, E.A., Batista, I.S., de Paula, E.R., Fritts, D.C., Sobral, J.H.A., 2009. Gravity wave initiation of equatorial spread/plasma bubble irregularities based on observational data from the SpreadFex campaign. *Ann. Geophys.* 27, 2607–2622. <http://dx.doi.org/10.5194/angeo-27-2607-2009>.
- Alfonsi, L., Spogli, L., Pezzopane, M., Romano, V., Zuccheretti, E., De Franceschi, G., Cabrera, M.A., Ezquer, R.G., 2013. Comparative analysis of spread-F signature and GPS scintillation occurrences at Tucumán, Argentina. *J. Geophys. Res. Space Phys.* 118, 4483–4502. <http://dx.doi.org/10.1002/jgra.50378>.
- Basu, S., Kelley, M.C., 1979. A review of recent observations of equatorial scintillations and their relationship to current theories of F region irregularity generation. *Radio Sci.* 14, 471–485. <http://dx.doi.org/10.1029/RS014i003p00471>.
- Bertoni, F.C.P., Sahai, Y., Raulin, J.P., Fagundes, P., Pillat, R.V.G., Gimenez de Castro, C.G.W., Lima, L.C., 2011. Equatorial spread-F occurrence observed at two near equatorial stations in the Brazilian sector and its occurrence modulated by planetary waves. *J. Atmos. Solar Terr. Phys.* 73, 457–463. <http://dx.doi.org/10.1016/j.jastp.2010.10.017>.
- Bhaneja, P., Earle, G.D., Bishop, R.L., Bullett, T.W., Mabie, J., Redmon, R., 2009. A statistical study of midlatitude spread F at Wallops Island, Virginia. *J. Geophys. Res.* 114, A04301 <http://dx.doi.org/10.1029/2008JA013212>.
- Bowman, G.G., 1995. Short-term delays in ionogram-recorded equatorial spread F occurrence of equatorial spread F. *Ann. Geophys.* 11, 624–633.
- Bowman, G.G., 1998. Short-term delays (hours) of ionospheric spread F occurrence at a range of latitudes, following geomagnetic activity. *J. Geophys. Res.* 103, 11627–11634. <http://dx.doi.org/10.1029/98JA00630>.
- Cabrera, M.A., Pezzopane, M., Zuccheretti, E., Ezquer, R.G., 2010. Satellite traces, range spread-F occurrence, and gravity wave propagation at the southern anomaly crest. *Ann. Geophys.* 28, 1133–1140. <http://dx.doi.org/10.5194/angeo-28-1133-2010>.
- Chandra, H., Rastogi, R.G., 1972. Equatorial spread-F over a solar cycle. *Ann. Geophys.* 28, 709–716.
- Chandra, H., Sharma, Som, Abdu, M.A., Batista, I.S., 2003. Spread-F at anomaly crest regions in the Indian and American longitudes. *Adv. Space Res.* 31, 717–727. [http://dx.doi.org/10.1016/S0273-1177\(03\)00034-6](http://dx.doi.org/10.1016/S0273-1177(03)00034-6).
- Fagundes, P.R., Abalde, J.R., Bittencourt, J.A., Sahai, Y., Francisco, R.G., Pillat, V.G., Lima, W.L.C., 2009. F layer postsunset height rise due to electric field prereversal enhancement: 2. Traveling planetary wave ionospheric disturbances and their role on the generation of equatorial spread F. *J. Geophys. Res.* 114, A12322 <http://dx.doi.org/10.1029/2009JA014482>.
- Fejer, B.G., Scherliess, L., de Paula, E.R., 1999. Effects of the vertical plasma drift velocity on the generation and evolution of equatorial spread F. *J. Geophys. Res.* 104, 19859–19869. <http://dx.doi.org/10.1029/1999JA000271>.
- Hoang, T.L., Abdu, M.A., MacDougall, J., Batista, I.S., 2010. Longitudinal differences in the equatorial spread F characteristics between Vietnam and Brazil. *Adv. Space Res.* 45, 351–360. <http://dx.doi.org/10.1016/j.asr.2009.08.019>.
- Hysell, D.L., 2000. An overview and synthesis of plasma irregularities in equatorial spread F. *J. Atmos. Sol. Terr. Phys.* 62, 1037–1056. [http://dx.doi.org/10.1016/S1364-6826\(00\)00095-X](http://dx.doi.org/10.1016/S1364-6826(00)00095-X).
- Hysell, D.L., Burcham, J., 2002. Long term studies of equatorial spread F using the JULIA radar at Jicamarca. *J. Atmos. Solar Terr. Phys.* 64, 1531–1543. [http://dx.doi.org/10.1016/S1364-6826\(02\)00091-3](http://dx.doi.org/10.1016/S1364-6826(02)00091-3).
- Jiang, C., Yang, G., Liu, J., Yokoyama, T., Komolmis, T., Song, H., Lan, T., Zhou, C., Zhang, Y., Zhao, Z., 2016. Ionosonde observations of daytime spread F at low latitudes. *J. Geophys. Res. Space Phys.* 121, 12093–12103. <http://dx.doi.org/10.1002/2016JA023123>.
- Kelley, M.C., McClure, J.P., 1981. Equatorial spread-F: a review of recent experimental results. *J. Atmos. Terr. Phys.* 43, 427–435. [http://dx.doi.org/10.1016/0021-9169\(81\)90106-9](http://dx.doi.org/10.1016/0021-9169(81)90106-9).
- Kelley, M.C., 1989. *The Earth's Ionosphere. International Geophysics Series*, vol. 43. Academic Press, San Diego, Calif.
- Kelley, M.C., 2009. *The Earth's Ionosphere: Plasma Physics & Electrodynamics*. Academic Press, San Diego, Calif, pp. 142–152.
- Kelley, M.C., Ilma, R.R., Crowley, G., 2009. On the origin of pre-reversal enhancement of the zonal equatorial electric field. *Ann. Geophys.* 27, 2053–2056. <http://dx.doi.org/10.5194/angeo-27-2053-2009>.
- Klausner, V., Fagundes, P.R., Sahai, Y., Wrasse, C.M., Pillat, V.G., Becker-Guedes, F., 2009. Observations of GW/TID oscillations in the F2 layer at low latitude during high and low solar activity, geomagnetic quiet and disturbed periods. *J. Geophys. Res.* 114, A02313 <http://dx.doi.org/10.1029/2008JA013448>.
- Krall, J., Huba, J.D., Fritts, D.C., 2013. On the seeding of equatorial spread F by gravity waves. *Geophys. Res. Lett.* 40, 661–664. <http://dx.doi.org/10.1002/grl.50144>.
- Lee, C.C., Liu, J.Y., Reinisch, B.W., Chen, W.S., Chu, F.D., 2005. The effects of the pre-reversal drift, the EIA asymmetry, and magnetic activity on the equatorial spread F during solar maximum. *Ann. Geophys.* 23, 745–751. <http://dx.doi.org/10.5194/angeo-23-745-2005>.
- Lyon, A.J., Skinner, N.J., Wright, R.W., 1961. Equatorial spread-F at Ibadan, Nigeria. *J. Atmos. Terr. Phys.* 21, 100–119. [http://dx.doi.org/10.1016/0021-9169\(61\)90104-0](http://dx.doi.org/10.1016/0021-9169(61)90104-0).
- Maruyama, T., Matuura, N., 1984. Longitudinal variability of annual changes in activity of equatorial spread F and plasma bubbles. *J. Geophys. Res.* 89, 10903–10912. <http://dx.doi.org/10.1029/JA089iA12p10903>.
- Maruyama, T., 1988. A diagnostic model for equatorial spread F 1. Model description and application to electric field and neutral wind effects. *J. Geophys. Res.* 93, 14611–14622. <http://dx.doi.org/10.1029/JA093iA12p14611>.
- McDougall, J.W., 1997. *Canadian Advanced Digital Ionosonde Users Manual*. University of Western Ontario, Scientific Instrumentation Ltd.
- Narayanan, V.L., Sau, S., Gurubaran, S., Shiokawa, K., Balan, N., Emperumal, K., Sripath, S., 2014. A statistical study of satellite traces and evolution of equatorial spread F. *Earth, Planets Space* 66, 160. <http://dx.doi.org/10.1186/s40623-014-0160-4>.
- Ossakow, S.L., 1981. Spread-F theories-A review. *J. Atmos. Terr. Phys.* 43, 437–452. [http://dx.doi.org/10.1016/0021-9169\(81\)90107-0](http://dx.doi.org/10.1016/0021-9169(81)90107-0).
- Pezzopane, M., Zuccheretti, E., Bianchi, C., Scotto, C., Zolesi, B., Cabrera, M.A., Ezquer, R.G., 2007. The new ionospheric station of Tucumán: first results. *Ann. Geophys.-Italy* 50, 483–492. <http://dx.doi.org/10.4401/ag-4426>.
- Pezzopane, M., Zuccheretti, E., Abadi, P., de Abreu, A.J., de Jesus, R., Fagundes, P.R., Supnithi, P., Rungraengwajiake, S., Nagatsuma, T., Tsugawa, T., Cabrera, M.A., Ezquer, R.G., 2013. Low-latitude equinoctial spread-F occurrence at different longitude sectors under low solar activity. *Ann. Geophys.* 31, 153–162. <http://dx.doi.org/10.5194/angeo-31-153-2013>.
- Poole, A.W.V., 1985. Advanced sounding 1. The FMCW alternative. *Radio Sci.* 20, 1609–1616. <http://dx.doi.org/10.1029/RS020i006p01609>.

- Rama Rao, S.V.G., Rao, B.R., 1961. Equatorial spread F in relation to post-sunset height changes and magnetic activity. *J. Geophys. Res.* 66, 2113–2120. <http://dx.doi.org/10.1029/JZ066i007p02113>.
- Rastogi, R.G., 1977. Equatorial range spread F and high multiple echoes from the F region. *Proc. Indian Acad. Sci. Sect. A* 85, 230–235. <http://dx.doi.org/10.1007/BF03049485>.
- Ray, S., DasGupta, A., 2007. Geostationary L-band signal scintillation observations near the crest of equatorial anomaly in the Indian zone. *J. Atmos. Sol. Terr. Phys.* 69, 500–514. <http://dx.doi.org/10.1016/j.jastp.2006.09.007>.
- Saito, S., Maruyama, T., 2006. Ionospheric height variations observed by ionosondes along magnetic meridian and plasma bubble onsets. *Ann. Geophys.* 24, 2991–2996. <http://dx.doi.org/10.5194/angeo-24-2991-2006>.
- Sastri, J.H., Abdu, M.A., Batista, I.S., Sobral, J.H.A., 1997. Onset conditions of equatorial (range) spread F at Fortaleza, Brazil, during the June solstice. *J. Geophys. Res.* 102, 24013–24021. <http://dx.doi.org/10.1029/97JA02166>.
- Sobral, J., Abdu, M., Takahashi, H., Taylor, M., de Paula, E., Zamlutti, C., de Aquino, M., Borba, G., 2002. Ionospheric plasma bubble climatology over Brazil based on 22 years (1977–1998) of 630 nm airglow observations. *J. Atmos. Sol. Terr. Phys.* 64, 1517–1524. [http://dx.doi.org/10.1016/S1364-6826\(02\)00089-5](http://dx.doi.org/10.1016/S1364-6826(02)00089-5).
- Stephan, A.W., Colerico, M., Mendillo, M., Reinisch, B.W., Anderson, D., 2002. Suppression of equatorial spread F by sporadic E. *J. Geophys. Res.* 107 (A2) <http://dx.doi.org/10.1029/2001JA000162>.
- Su, S.Y., Liu, C.H., Ho, H.H., Chao, C.K., 2006. Distribution characteristics of topside ionospheric density irregularities: equatorial versus midlatitude regions. *J. Geophys. Res.* 111, A06305 <http://dx.doi.org/10.1029/2005JA011330>.
- Sultan, P.J., 1996. Linear theory and modeling of the Rayleigh-Taylor instability leading to the occurrence of equatorial F. *J. Geophys. Res.* 101, 26875–26891. <http://dx.doi.org/10.1029/96JA00682>.
- Tsunoda, R., 1985. Control of the seasonal and longitudinal occurrence of equatorial scintillations by the longitudinal gradient in the integrated E region Pedersen conductivity. *J. Geophys. Res.* 90, 447–456. <http://dx.doi.org/10.1029/JA090iA01p00447>.
- Tsunoda, R.T., 2008. Satellite traces: an ionogram signature for large scale wave structure and a precursor for equatorial spread F. *Geophys. Res. Lett.* 35, L20110 <http://dx.doi.org/10.1029/2008GL035706>.
- Upadhyaya, A.K., Gupta, S., 2014. A statistical analysis of occurrence characteristics of Spread-F irregularities over Indian region. *J. Atmos. Terr. Phys.* 112, 1–9. <http://dx.doi.org/10.1016/j.jastp.2014.01.019>.
- Wang, G.J., Shi, J.K., Wang, X., Shang, S.P., Zhrebtsov, G., Pirog, O.M., 2010. The statistical properties of spread F observed at Hainan station during the declining period of the 23rd solar cycle. *Ann. Geophys.* 28, 1263–1271. <http://dx.doi.org/10.5194/angeo-28-1263-2010>.
- Whalen, J.A., 2002. Dependence of the equatorial bubbles and bottomside spread F on season, geomagnetic activity and $E \times B$ drift velocity during solar maximum. *J. Geophys. Res.* 107, 1024. <http://dx.doi.org/10.1029/2001JA000039>.
- Zhu, Z., Lan, J., Luo, W., Sun, F., Chen, K., Chang, S., 2015. Statistical characteristics of ionogram spread-F and satellite traces over a Chinese low-latitude station Sanya. *Adv. Space Res.* 56, 1911–1921. <http://dx.doi.org/10.1016/j.asr.2015.03.038>.